JOURNAL OF GEOPHYSICAL RESEARCH, VOL. 113, C12016, doi:10.1029/2007JC004678, 2008

Mid-depth internal wave energy off the Iberian Peninsula estimated from seismic reflection data

G. Krahmann,[1] P. Brandt,[1] D. Klaeschen,[1] and T. Reston[1,2]

Received 6 December 2007; revised 29 August 2008; accepted 18 September 2008; published 17 December 2008.

[1] Energy levels of internal waves are estimated from seismic reflection data. Three legacy seismic sections from 1993 and 1997 obtained off the Iberian Peninsula have been analyzed for acoustic reflections within the water column. The reflections are aligned continuously for up to several kilometers over large parts of the sections and in the depth interval from 200 to 2000 m. Depth variations of these reflections are thought to be caused by the background internal wave field. From the variations we derive horizontal wave number spectra of normalized internal wave displacement. The general slope of the power density spectra is remarkably consistent for all sections and agrees well with model spectra for internal waves. Significant differences within the sections can be found when sufficiently large subsections are averaged. The spatial variation of the energy level indicates increasing internal wave activity with shallower water depths as well as near a subsurface eddy.

Citation: Krahmann, G., P. Brandt, D. Klaeschen, and T. Reston (2008), Mid-depth internal wave energy off the Iberian Peninsula estimated from seismic reflection data, *J. Geophys. Res.*, *113*, C12016, doi:10.1029/2007JC004678.

1. Introduction

[2] Seismic reflection data has recently been discovered to contain information of interest to physical oceanographers [*Holbrook et al.*, 2003]. Analysis of a seismic data set, collected off Norway together with expendable temperature and salinity probes, confirmed that step-like vertical temperature variations of more than a few hundredths of a degree over a few meters are reflective to the sound used in marine seismic observations [*Nandi et al.*, 2004]. Depending on the sign of the temperature change these reflections may undergo a 180° phase change or not. The reflections within the water column have frequently been found to occur in the form of more or less continuous horizontal or slightly sloping reflected phases that are related to layering in the water [*Holbrook et al.*, 2003]. Such layers and thus the reflections are often observed to be stable over time-spans much longer than internal wave periods, otherwise a continuous tracking over sometimes dozens of kilometers would not be possible [*Johannessen and Lee*, 1974; *Merryfield*, 2002]. One can interpret their depth variations over limited horizontal scales (up to a few kilometers) observed with seismic methods as depth variations of isopycnals caused by internal waves [*Holbrook and Fer*, 2005] and apply methods originally developed for specialized hydrographic observations of internal waves [*Katz and Briscoe*, 1979].

[3] From standard hydrographic measurements we know that vertical temperature variations in the form of jumps or steps are found in many parts of the world's oceans. A number of processes can lead to such locally elevated vertical gradients of temperature. Among them are double diffusion and interleaving of water masses. Compared to these processes, the strain associated with internal waves and subinertial motions results in only weak variations of the background temperature gradient. However, due to associated horizontal and vertical motions, internal waves and subinertial motions are able to distort existing surfaces of strong temperature gradients. Common to these processes are vertical scales of 1 to 100 m, which classifies them as oceanic fine-structure. Seismic measurements alone are not likely to be able to distinguish between the different processes, something that will be possible with contemporaneous hydrographic observations. Nevertheless legacy seismic data that typically lacks accompanying hydrographic measurements contains valuable information. If the depth variations of reflectors are assumed to be similar to the vertical displacement of isopycnals they can be used to calculate the strength of the internal wave field at different wavelengths [*Garrett and Munk*, 1975; *Katz and Briscoe*, 1979; *Holbrook and Fer*, 2005]. The spectral density of the vertical displacement variance in horizontal wave number space is then, after normalization for the strength of the local stratification, a measure of the available potential energy of the internal wave field [*Katz and Briscoe*, 1979; *Holbrook and Fer*, 2005]. The accuracy of this measure is somewhat limited by assumptions and constraints of the seismic method and processing. Stationarity is of course not given in the oceanic environment. A propagating internal wave can move by a significant fraction of its wavelength during the time over which seismic data is collected at a single midpoint location. The effect will be a smoothing of the reflector displacements. The frequency and bandwidth

[1] Leibniz-Institut für Meereswissenschaften an der Universität Kiel, IFM-GEOMAR, Kiel, Germany.
[2] Now at University of Birmingham, Birmingham, UK.

0148-0227/08/2007JC004678$09.00

of the seismic source signal will also have an impact on the horizontal resolution of the seismic measurements with lower frequencies leading to a lower resolution. Both points will cause apparent reductions of the internal wave energies. Despite these, *Holbrook and Fer* [2005] showed that displacement spectra determined from seismic data compare well with the Garrett-Munk model for ocean internal waves suggesting that the observed displacements might not be lowered by much.

[4] In this study we examine data collected in the region west of the Iberian Peninsula, a location that is particularly well suited for seismic oceanography. Mediterranean Water (MW) leaves the Mediterranean Sea and enters the North Atlantic through the Strait of Gibraltar (Figure 1). MW flows downslope from the strait's sill (300 m depth) to its neutral density level at about 1000 m while entraining ambient Atlantic Water. It then turns to follow the continental slope north- and westward as Mediterranean Undercurrent [e.g., *Bower et al.*, 1997]. At the southwestern corner of the peninsula, Cape St. Vincent, it turns again northward. In the vicinity of the Cape and further north at the Estremadura Promontory the undercurrent episodically detaches from the slope and forms eddies, dubbed Meddies because of the origin of their core's water mass [*Bower et al.*, 1997].

[5] Both the undercurrent and the Meddies are relevant for seismic oceanography. Relative to the surrounding Atlantic water masses, the MW is both warm and saline. These differences set up an environment favorable for interleaving between the two water masses and also for double diffusive processes, in which the differing molecular diffusivities of heat and salt lead to characteristic thermohaline steps [e.g., *Magnell*, 1976]. The result is a large number of vertical temperature and salinity steps between the interleaving layers and also, due to double diffusive processes, above and beneath the Meddies. The temperature steps are typically large enough, a few hundredths of a degree over only a few meters, to be seen as reflecting features in seismic data. Since the double diffusive processes are rather slow, the layers are quite stable and under certain circumstances can even exist for years [*Johannessen and Lee*, 1974].

[6] In the following we first describe the seismic data used in this study and outline its processing. Then we lay out the methods used to estimate the internal wave energy levels. The results of our analyses are shown in the subsequent section and summarized and discussed thereafter.

2. Data

[7] Seismic reflection data from three seismic sections were reprocessed and analyzed for this study (Please note that in this manuscript we follow oceanographic convention and use the term *profile* for a one dimensional measurement or data set along the vertical (depth) axis and *section* for a set of horizontally consecutive profiles. The respective seismic terms would be *gather* and *profile*, respectively.). One section (IAM-4), collected in summer 1993 as part of the Iberian Atlantic Margin (IAM) experiment [e.g., *Banda et al.*, 1995], cuts in a southeasterly direction across Gorringe Bank off the southwestern edge of the Iberian Peninsula (Figure 1). The two other sections were collected as part of the Iberia Seismic Experiment (ISE) in summer 1997 and are located further to the north [*Pérez-Gussinyé et al.*, 2003]. No exactly contemporaneous hydrographic measurements exist for either data set, although a hydrographic section (World Ocean Circulation Experiment section A25) was measured within 14 days and at a distance of 30 nautical miles from and approximately parallel to one of the ISE sections. While this is not sufficient for a quantitative comparison we were able to assess the general hydrographic structure. Sharp vertical gradients in acoustic impedance (the product of sound speed and density), which cause seismic reflections, are visible in the hydrographic data at the bottom of the surface mixed layer and in the depth interval between 500 and 2000 m (Figure 2). Particularly strong impedance gradients are found above and below the intermediate sound speed maximum at about 1100 m characterizing the center depth of the MW layer. Our analysis of the hydrographic data showed that more than 90% of the reflection amplitudes were caused by changes in sound speed and not by changes in density (Figure 2). We also found that, for our data sets, the sound speed changes were mostly due to variations in the temperatures.

[8] The seismic data were collected with multichannel hydrophone streamers towed behind seismic vessels. For the IAM-4 line 192 hydrophone channels were located every 25 m over a distance of 4775 m and for the ISE lines 164 channels every 25 m over a distance of 4075 m. While the vessels were slowly advancing (at about 4 knots), pressure pulses were emitted by the release of compressed air from airguns into the water column every 75 m for the IAM-4 line and every 100 m for the ISE lines. Sound waves returning from reflectors in the water column and below the seafloor were recorded along the hydrophone streamers. Seismic data processing included the removal of the direct water wave, gain recovery, source signature deconvolution, and amplitude calibration. For the removal of the direct wave several methods like Frequency-wave number (F-K filter), Karhunen-Loeve filter (K–L filter or Eigen-vector filter) exist. In this data set we removed the direct wave by linear Radon transformation (Tau-P) in the shot-gather domain. The direct wave was extracted with forward transformation to Tau-P domain, muting of non-direct wave events, and backward transformation to the original space-time (x, t) domain. The extracted (modeled) direct wave was subsequently subtracted from the original data after an amplitude matching procedure in the sense of a least-squares fit. For each time sample a factor was computed that matches the amplitudes of the modeled and original traces over a sliding time window. Before subtraction, the modeled trace was multiplied by the estimated factors. The amplitude matching procedure before subtraction is more important than the method of the removal method itself especially if laterally amplitude variations from trace to trace exist. To maintain a ''true'' amplitude reflection response of the reflectors in the water column, a source signature deconvolution was applied for each shot-gather to account for the source components of the source wavelet. An additional amplitude calibration based on the relations of the seafloor and the water column multiple of the seafloor events [*Warner*, 1990] allowed an interpretation of absolute reflection coefficients for detailed analysis.

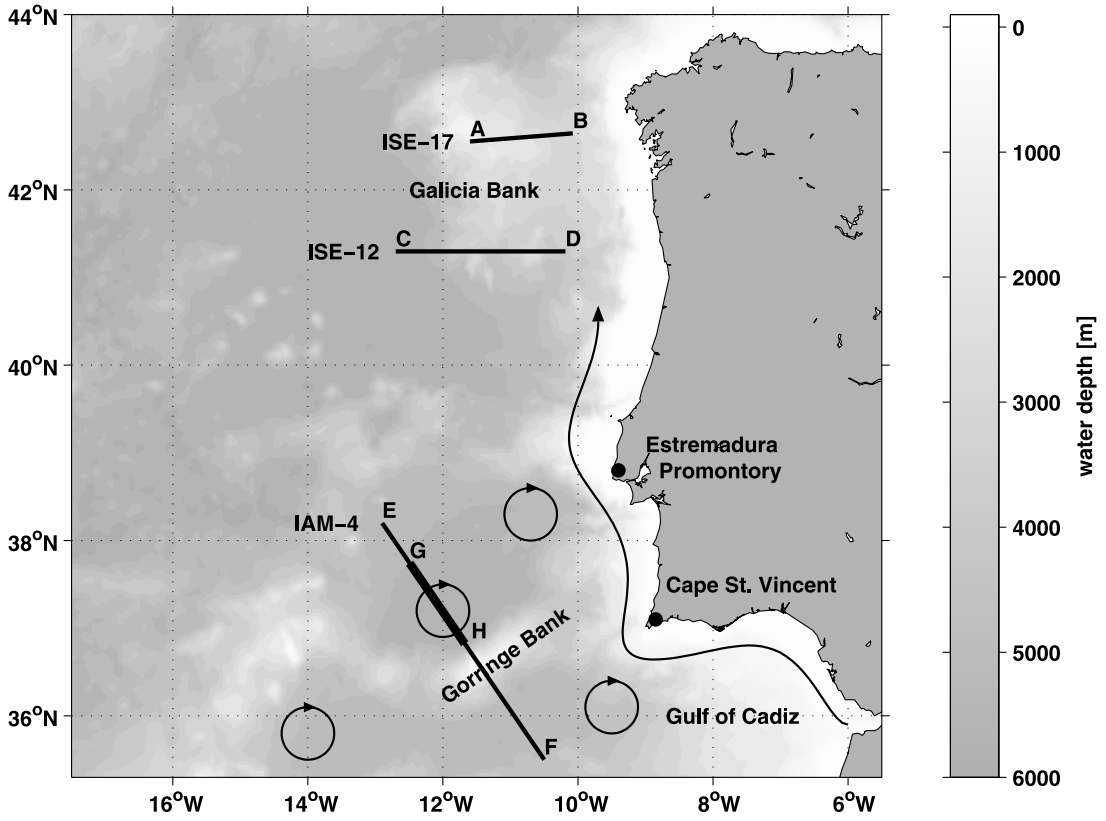

Figure 1. Bathymetry west of the Iberian Peninsula showing the location of the three sections analyzed in this study. Labels corresponding to the sections can also be found in Figures 3, 4, and 8. Also shown are an idealized spreading pathway of Mediterranean Water along the continental slope and idealized Meddies, including one at the observed location in the southernmost section.

[9] Starting from a climatological sound speed profile (based on *Levitus and Boyer* [1994]) from the area of acquisition, the sound speed profile was updated iteratively by prestack depth migration and residual moveout analysis to get the final seismic images in depth [*Guo and Fagin*, 2002]. Only at the location of a Meddy in section IAM-4, the migration analysis required a significant deviation of up to 30 m/s from the climatological sound speed profile. The resulting reflectivity images are shown in Figures 3 and 4 (the last graph also shows the sound speed estimate at the Meddy's location). The sections consist of seismic traces spaced 12.5 m (25 m for IAM4) apart, which are the vertical profiles used in the subsequent analyses.

[10] Extensive areas with water column sound reflections are present in all three sections. Continuous reflectors can be identified in the depth interval from about 200 to 2000 m with the strongest reflections typically between 700 and 1500 m. Above 200 m the direct arrival of the seismic sound at the streamer's hydrophones is too strong and masks any reflections within the upper part of the water column. Below about 2000 m the weak and only gradual vertical temperature variations of the different North Atlantic Deep Water components do not sufficiently reflect the sound to be visible in the seismic data.

[11] A particularly interesting feature found in the seismic data was a Meddy in section IAM-4 (Figure 4, bottom). A clearly visible core with only a few reflective layers is surrounded by nearly continuous reflectors above and beneath and between a large number of smaller structures on either side. From the horizontal dimension of the structure of 50 to 70 km that is comparable to typical diameters of Meddies of 50 to 100 km, we infer that the Meddy was cut fairly close to its central axis. The long reflectors steepen considerably close to the sides of the Meddy. Maximum observed slopes on its lower side are about 0.040. We found such high values however only near the Meddy's sides over a horizontal interval of less than 5 km. Such steep reflectors would thus be difficult to capture with the typical horizontal resolution of conventional hydrographic observations. The slopes underneath most of the Meddy range from 0.008 to 0.015. These values are somewhat steeper than the slopes of interleaving layers of 0.0057 ± 0.0025 previously reported by *May and Kelley* [2002] for Meddy Sharon and derived from conventional hydrographic data. That Meddy was however, at the time of their observation, quite distant from the formation regions, and must thus have undergone significant transformation and decay. Unfortunately, because of the lack of accompanying hydrographic measurements, we are not able to determine the slopes of the reflective layers relative to isopycnals which would be a dynamically relevant property. *May and Kelley* [2002] report that the isopycnals near Meddy Sharon sloped about half as much as the interleaving layers.

3. Methods

[12] The basic information used in this study is the variation of the depth of reflectors at which sound from

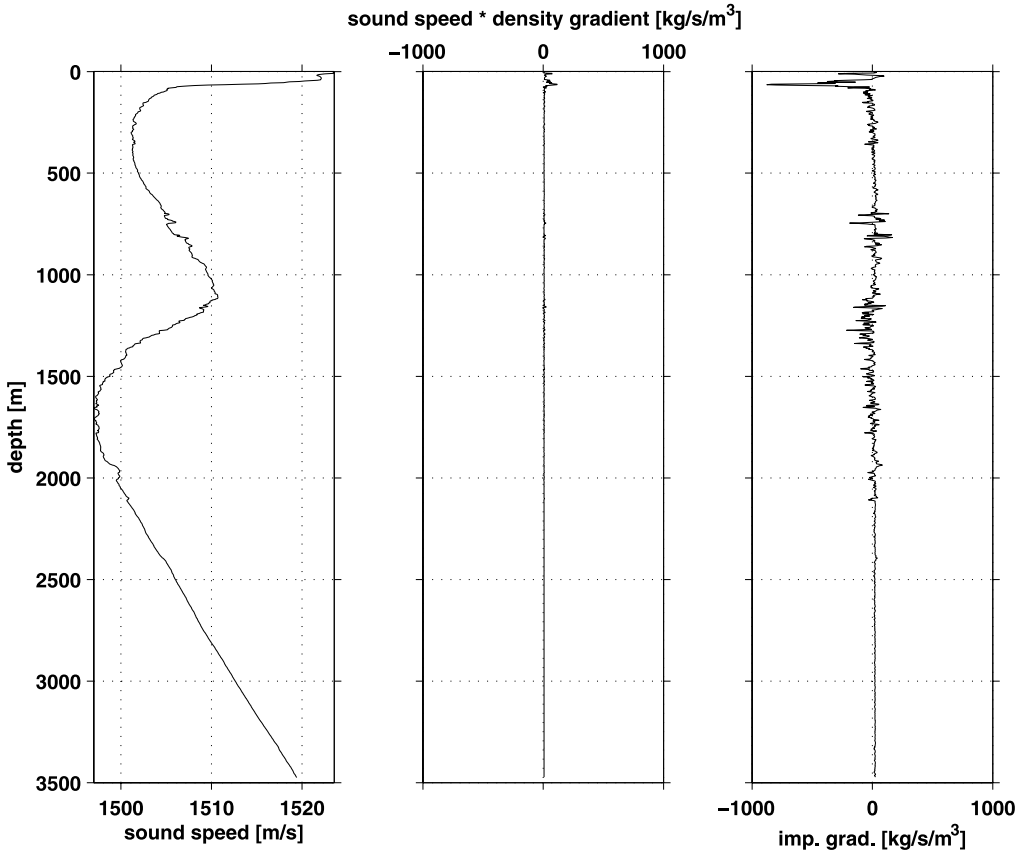

Figure 2. Sound speed, the product of sound speed and vertical gradient of density, and the vertical gradient of acoustic impedance for station 11 of World Ocean Circulation Experiment section A25 collected within 14 days and at a distance of 30 nautical miles to seismic section ISE-12. The middle and right graphs are displayed at the same scale and highlight that the vertical density gradient contributes only to a minor degree to the acoustic reflectivity.

the seismic sources was reflected within the water column. To extract the depths of laterally continuous reflectors from the seismic data we applied a 3-step algorithm consisting of the identification of reflections in each profile (each a trace from the prestack depth migrated section); the lateral tracking of reflectors; and the retention of only sufficiently long and reflective tracks. In the first step (Figure 5, left) all possible sound reflections are gathered by examining the profile for its strongest peaks that also have a shape similar to that of the source signal (a characteristic negative-positive-negative sound pressure triplet, Figure 5, left). To accomplish this the profile is repeatedly examined for the highest peak, which then is cross-correlated with the source signal to locate the depth of the reflection. Second order interpolation is used to determine the exact depth of the peak. A source signal-long interval of the profile centered at the identified peak is blanked out (dashed parts of the signals in Figure 5, left) and the search for the highest peak starts again. Repeating these steps up to, in our case, thirty times gives us the depths of all possible peaks within each profile. The number thirty is simply the upper limit of vertically separate peaks and depends only on the length of the source signal, the vertical resolution of the seismic data, and the water depth.

[13] In the second step we identify horizontally continuous reflectors; i.e., we look for horizontally aligned peaks. We start by picking a peak in the first profile. Then the neighboring profile is inspected for peaks that match the depth of the original peak to within 10 m. This maximum allowed vertical deviation between neighboring peaks limits the slope of reflectors to values below about 1 for the ISE sections or 0.5 for the IAM section, respectively. If we find such a peak, it is assigned to the same reflector. If no such peak exists, we examine the following two profiles. Consequently gaps of up to two profiles (25 or 50 m) are permitted within a reflector (for further calculations such gaps are linearly interpolated). If we find such an aligned peak, the identification process is continued in the adjacent profile using the just recognized peak as the starting point. If no aligned peaks can be found over three consecutive profiles we declare the reflector ended and go back to the next unassigned peak. This process is continued until all peaks have been assigned to a reflector.

[14] As a third step only reflectors with continuously aligned peaks in more than 64 neighboring profiles are retained. This ensures that only long continuous reflectors that are likely created by physical features and not by random noise are used in the subsequent analysis. In our

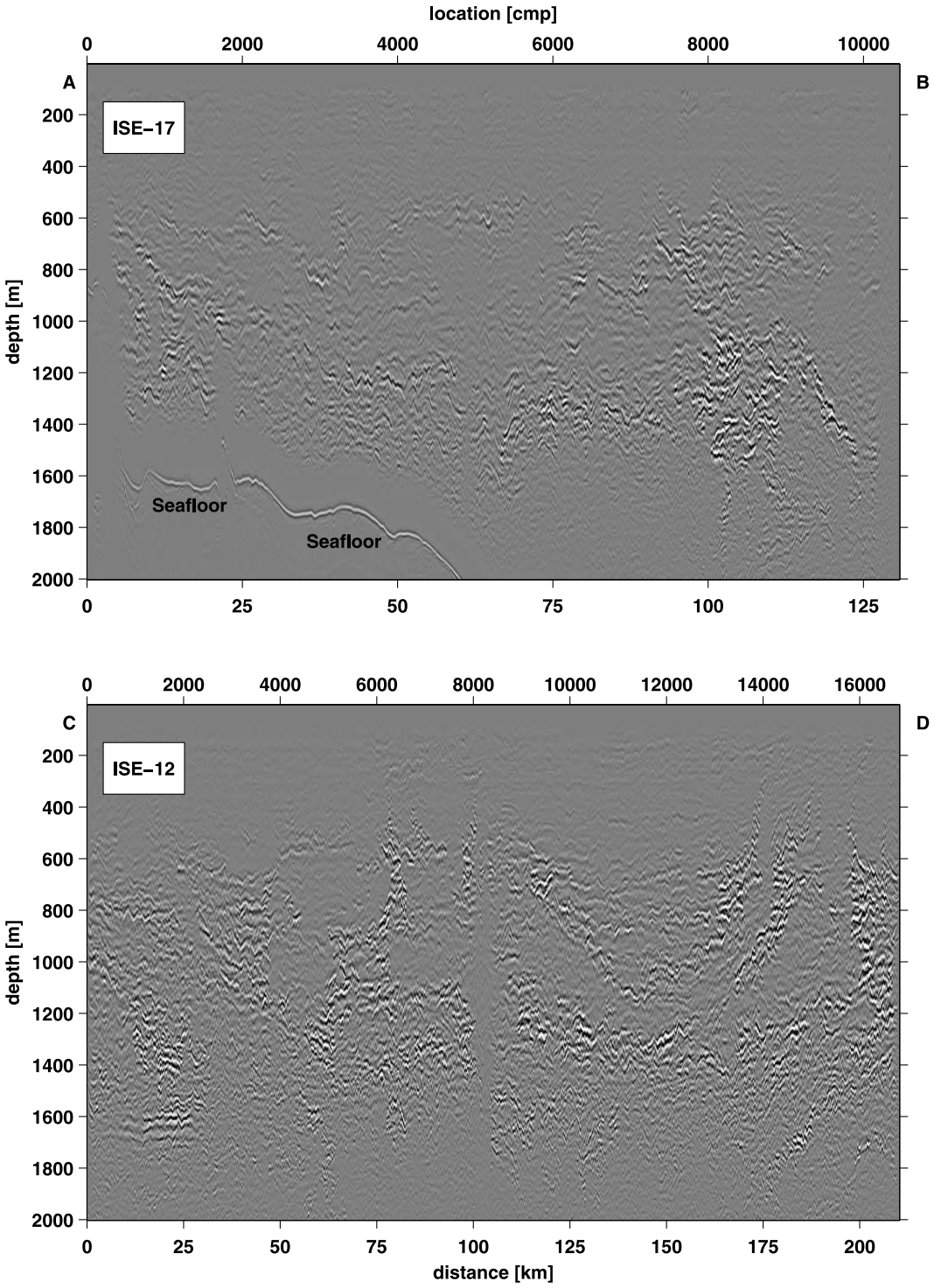

Figure 3. Sound reflectivity for sections ISE-17 and ISE-12. Lighter (darker) regions denote positive (negative) downward gradients of acoustic impedance. Labels on the top left and right of each graph denote the start and end locations from each section and correspond to those introduced in Figure 1.

case all reflectors longer than 64 profiles were cut into 64-point long pieces as we identified too few longer reflectors to result in meaningful spectral data. Cutting the reflectors also simplified the calculation of the spectra and their uncertainties. The length at which one decides to cut off long reflectors depends of course on the data set that is being analyzed. Figure 5 (right) shows as an example a portion of section ISE-12. Shaded in gray is the reflectivity, with solid undulating lines indicating the tracked reflectors. The vertical line with the three dots marks the profile (seismic trace) with the identified peaks from Figure 5 (left).

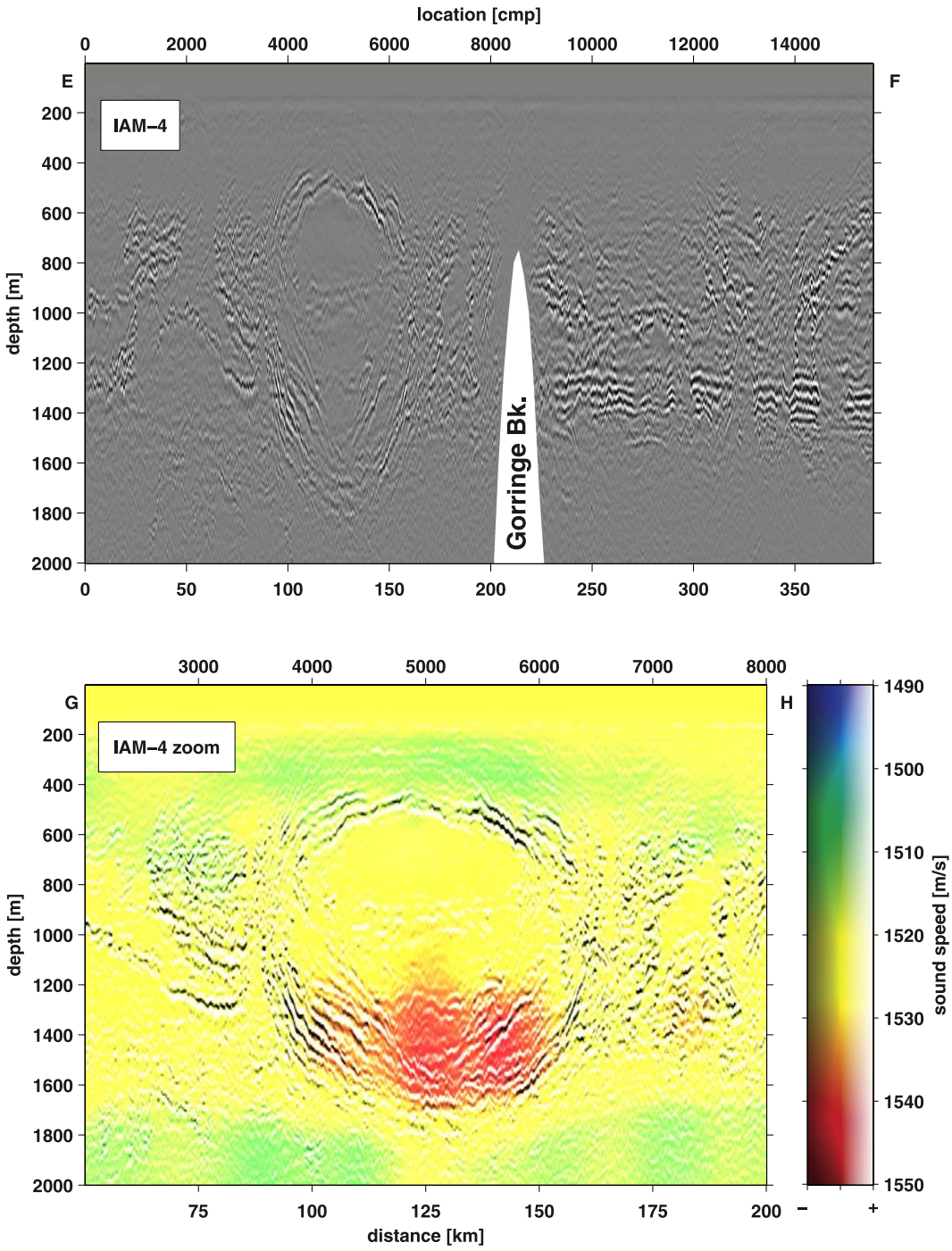

Figure 4. Sound reflectivity of (top graph) section IAM-4 as in Figure 3. Also shown in the bottom graph is a magnified part of section IAM-4 where a Meddy is intersected. In this graph the sound velocity as estimated from the migration analysis is given by the color shading.

[15] This method is independent of the actual strength of the reflection and thus identifies reflectors from their continuity; in a way similar to visual inspection after applying a very high gain setting in conventional seismic analyses. To increase the amount of data underlying the subsequent spectral analyses, we applied the algorithm both to positive and negative phase reflections as they are caused by physically independent positive or negative jumps in the sound speed.

[16] Power densities of the vertical displacement wave number spectra were calculated for all 64-point long reflectors using Welch's averaged modified periodogram method with a 64-point wide Hanning window and no overlap. Prior to the spectral calculation, the average depths of the reflectors were subtracted. As explained above we refrained from calculating spectra for longer spatial wavelengths, as there were too few to produce statistically meaningful data. For our data the analyzed 64-point long coherent reflectors

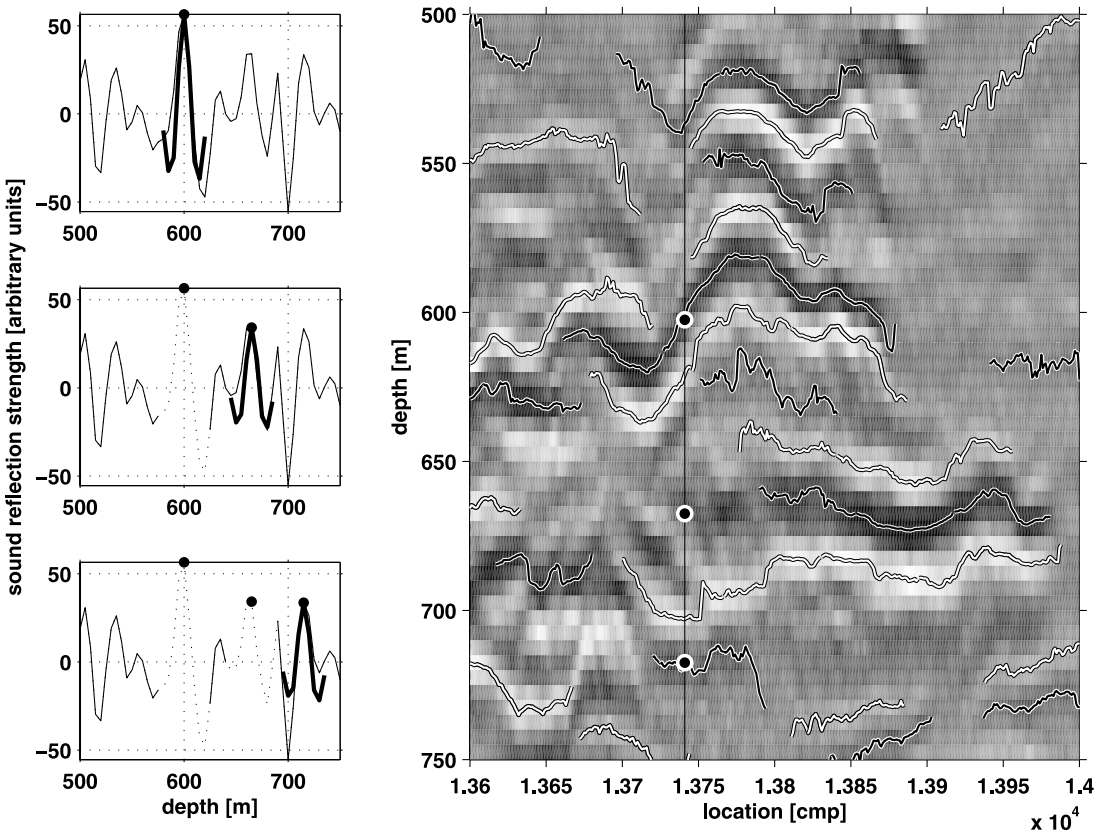

Figure 5. Example analysis for the tracking algorithm. The left graph shows a reflectivity profile (a single trace extracted from the migrated seismic section) and the method used to identify reflective peaks. In the right graph a subset of section ISE-12 is shown with the same profile highlighted by a thin vertical line. The three dots mark the peaks identified in the left graph. The more or less undulating lines show tracked reflectors that continued over at least 64 neighboring profiles. Note that one of the three identified peaks is not located on a tracked reflector. Even though there were neighboring peaks, they did not extend over more than 64 profiles. These peaks were thus not retained for the spectral analysis.

with profiles every 12.5 m (25 m for IAM-4) translate into horizontal wave numbers of the spectra from 1.25 to 40 km^{-1} (0.625 to 20 km^{-1}) or wavelengths from 25 to 800 m (50 to 1600 m). The average depth and lateral position of the reflector are used when considering spatial variations.

[17] For a given wave energy, vertical displacements by an internal wave vary with the vertical density gradient [*Katz and Briscoe*, 1979]. We thus had to correct for this effect to create comparable spectra. Like *Holbrook and Fer* [2005] we therefore normalized the displacement power spectral densities by multiplying with the vertically varying buoyancy frequency (the frequency at which a vertically displaced water parcel oscillates around its equilibrium depth). In the absence of truly contemporaneous salinity and temperature measurements we derived a buoyancy frequency profile from climatological temperature and salinity profiles of the region [*Levitus and Boyer*, 1994] and from the temporally and spatially close sections A03 and A25 of the World Ocean Circulation Experiment. For the depth range from 700 to 1500 m where most reflections were located only little variation was found between the different data sets and the buoyancy frequency in that range deviated not more than 20% from the value for 1000 m of about 1.4 cycles per hour (1 cycle per hour = $2\pi/3600$ s^{-1}).

4. Results

[18] As all derived spectra are based on only a single 64-point long reflector, they are relatively noisy. To obtain statistically meaningful values we averaged all single-reflector spectra within the depth interval from 700 to 1500 m of each section. The three section-average spectra and their uncertainties are indicated by triplets of lines in Figure 6 and are compared to the towed wave number spectrum after Garrett and Munk (GM76 [*Katz and Briscoe*, 1979]). The uncertainty of the average spectra in Figure 6 depends on the number of independent spectra that are averaged. Since the vertical excursions of the reflectors are often coherent over several vertically neighboring reflectors and thus not statistically independent, we reduced the number of independent samples in the uncertainty calculation by a factor of 6. This factor was estimated from an analysis of the vertical coherence of the reflector displacements. In Figure 7 we show the correlation of the reflector displacement as a function of the vertical distance between the reflectors. We find that the 95% significant correlation

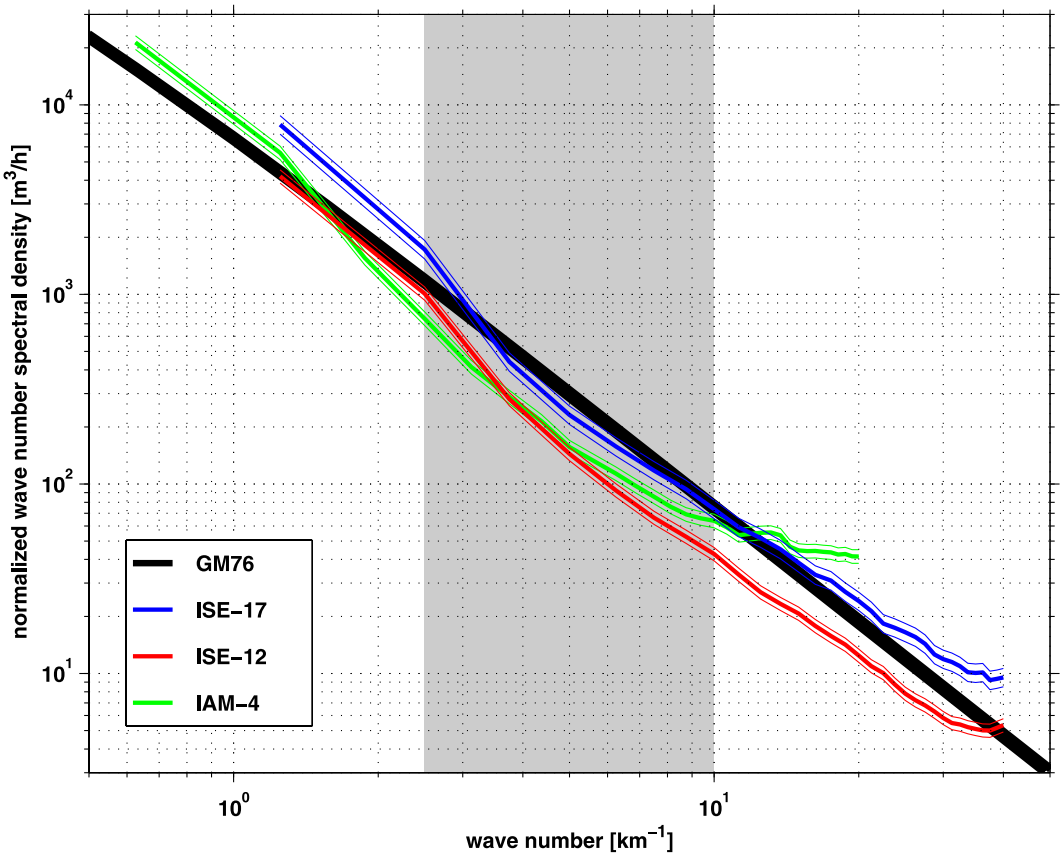

Figure 6. Average normalized wave number power spectral densities of reflector displacement and their uncertainties from the three sections analyzed in this study. Also shown is the internal wave spectrum expected for open ocean conditions [*Garrett and Munk*, 1975; *Katz and Briscoe*, 1979] for the latitude range of the three sections and for a buoyancy frequency of 1.4 cycles per hour. The shaded area denotes the wave number interval over which we integrated the spectra to compare energy levels.

level is crossed at about 75 m distance. Using a minimum distance between tracked reflectors of 15 m, i.e. the width of the source signal peak, we get a maximum of 6 correlated tracked reflectors. Typically there were fewer than 6 reflectors within any 75 m depth interval so that the number of 6 represents a conservative estimate.

[19] Inspection of Figure 6 shows that the general slopes of the average spectra of the three sections are fairly similar and agree quite well with GM76. At wave numbers larger than about 10 cycles per km for IAM-4 and 25 cycles per km for the ISE sections the spectra start to level off, indicating the influence of noise and the limited vertical resolution of the seismic data. The overall shape of the average spectrum is remarkably consistent between the three sections and also between any selected smaller parts of the sections (not shown). It also agrees well with the spectra found by *Holbrook and Fer* [2005] off the Norwegian coast.

[20] While the shape of the spectra is so consistent and the three section averages agree to a good degree, we found some variability at smaller horizontal scales. We did not find any significant peaks in the spectra but could distinguish different levels of the spectra or, in other words, found variations in the internal wave energy. We calculated a representative value for the energy content of the spectra by integrating over the interval of wave numbers from 2.5 to 10 cycles per km or wavelengths from 100 to 400 m (shaded part in Figure 6). This particular interval was chosen to cut out the high wave numbers, which had shown noise effects, and the low wave numbers, where sloping isopycnals might influence the calculation. To examine the spatial variation of the level of the energy content (in the following simply energy level) we averaged the data over 600 profile wide boxes, i.e., 7.5 km for the ISE sections and 15 km for the IAM-4 section (Figure 8). Even after averaging over the several hundred spectra contained in each box, the uncertainty of the average energy levels (shaded ranges in Figure 8) still remained fairly large. To obtain statistically significant differences we had to average further over even larger parts of the sections. Blue and green bars and the attached numbers in Figure 8 denote the subsections we chose. Their energy levels are listed in Table 1.

[21] As already shown in Figure 4, section IAM-4, which is cut in half by Gorringe Bank, intersects a Meddy in its northwestern (Figure 8, left, lower graph) half. We find that the side of the section containing the Meddy (blue bar, label 7) is characterized by a significantly higher energy level

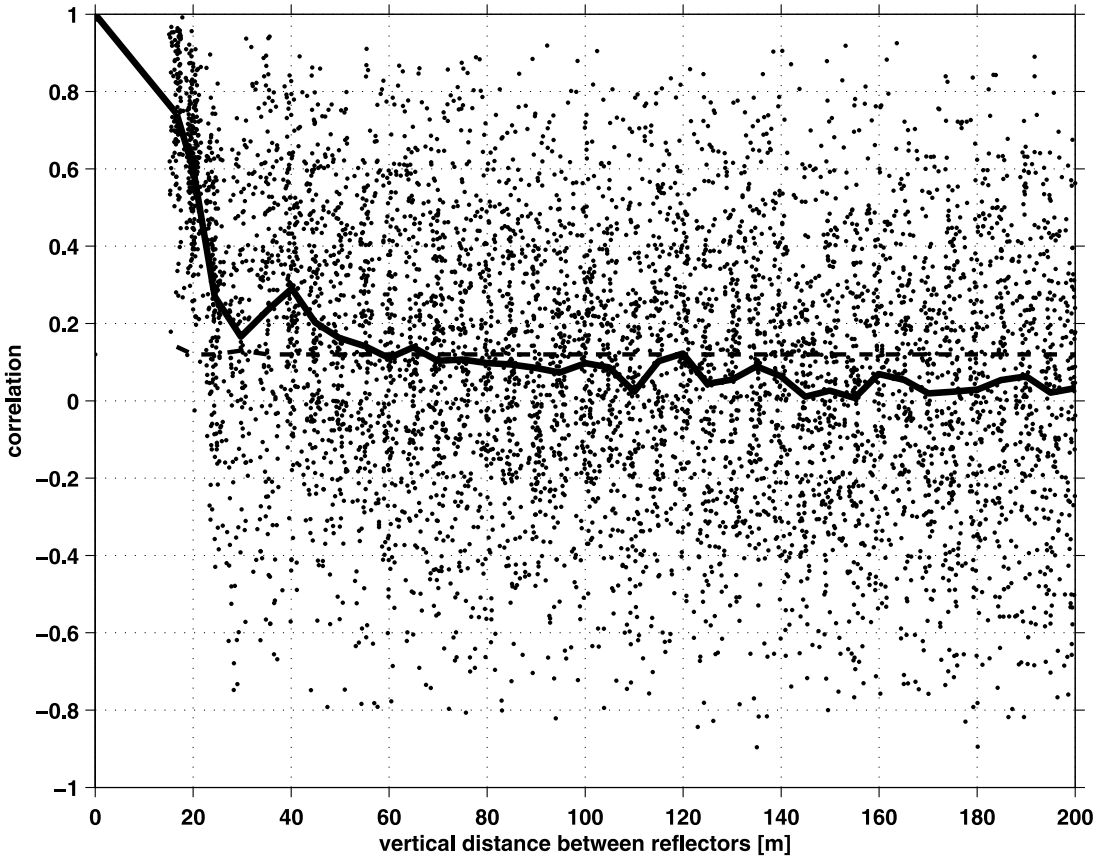

Figure 7. Correlation between the vertical excursion of tracked reflectors as a function of the vertical distance between the reflectors. The solid line shows the average correlation calculated over 5 m intervals and the dashed line indicates the 95% significance level. Only reflectors that overlapped by more than 50 points were used in this analysis. The tracked reflectors were detrended before to avoid enhanced correlation levels due to the large scale stratification. We find that at vertical distances of more than about 75 m the vertical excursions of the reflectors are no longer significantly correlated.

than the southeastern side. The higher energy level extends however not only over the Meddy center and its immediate surroundings but is present throughout the whole half of the section. This suggests that the elevated energy level might not be an artifact of the Meddy's interleaving with the surrounding water masses but could indeed be elevated internal wave activity north of Gorringe Bank.

[22] The two sections of the 1997 ISE experiment located further to the north cut across a different bathymetric regime. Section ISE-12 crosses a variable topography with two parts of Galicia Bank rising up to 2800 and 2200 m, respectively, while the other parts of the section are deeper than 3500 m. Our analysis shows elevated levels of energy over the subregions with shallower and/or rougher topography. We find that the differences in the energy levels are significant only when averaged over the four larger subregions that cover the deep and the shallow parts of the section (Figure 8, middle).

[23] ISE-17, only 130 km further to the north and the northernmost section analyzed here, is fully located to the east of Galicia Bank. It is also the shallowest of the analyzed three sections with a maximum depth of only 2600 m, shallowing toward the Galicia Bank to the west. The spatial distribution of internal wave energy in section ISE-17 shows a significant variation between its deeper and its shallower halves, again with the shallower side being more energetic.

[24] Overall we find variations of the internal wave energy level that coincide with two different hydrographic and bathymetric variations. Sections ISE-12 and -17 exhibit a correlation between the energy level and the water depth or possibly the roughness of the topography, which is rougher in shallower parts. We note that the relation between water depth and energy level also holds among the three sections when the Meddy's part of IAM-4 is excluded. A more than three-fold increase in energy level between the southern- and northernmost sections coincides with a water depth reduction from more than 4500 m to about 2000 m. A different energy level variation is found within section IAM-4. Energy levels differing by a factor of two are found between the opposite sides of Gorringe Bank. These cannot be explained by variations of the topography, which is similarly deep and flat on both sides of the bank. The presence of a Meddy on the higher-level side is, however, suggestive of a relationship between the Meddy

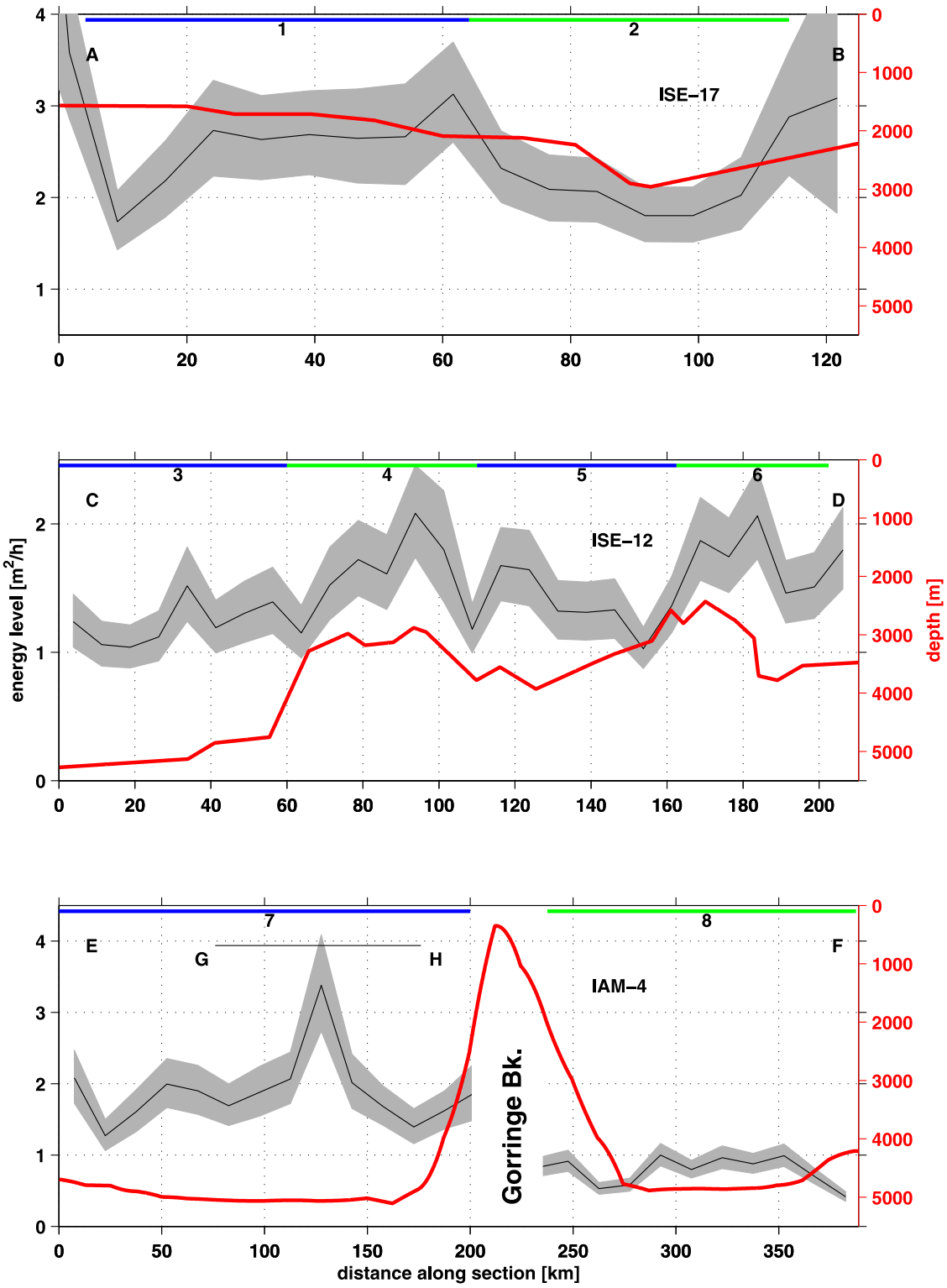

Figure 8. Horizontal variation of the internal wave energy level for the three seismic sections. Also included for each section is the water depth. The top shows section ISE-17, the middle shows section ISE-12, and the bottom shows section IAM-4 with the left half cutting through the Meddy already shown in Figure 4. The shaded areas indicate the uncertainty of the energy level estimates. Blue and green lines at the top of each figure denote parts of the respective section for which the average energy levels are given in Table 1. Letters corresponding to Figure 1 denote the start and end points of the sections.

Table 1. Integrated Internal Wave Energy Levels for Selected Parts of the Seismic Sections Shown in Figure 8[a]

Label	Section	Part (km)	Water Depths (m)	Energy Level (m^2/h)	Number of Reflectors
1	ISE-17	8–70	1600–2100	2.62 ± 0.17	1827
2	ISE-17	70–120	2100–2900	2.11 ± 0.16	1427
3	ISE-12	0–60	>4500	1.23 ± 0.08	2029
4	ISE-12	60–110	2800–3500	1.58 ± 0.11	1631
5	ISE-12	110–163	3300–4000	1.38 ± 0.09	1878
6	ISE-12	163–203	2200–3000	1.73 ± 0.13	1340
7	IAM-4	0–200	>4500	1.89 ± 0.09	3162
8	IAM-4	235–390	>4500	0.78 ± 0.04	3015

[a]The uncertainty of the estimate is derived from the 95% confidence intervals of the spectra.

and the internal wave field but remains to be confirmed by other data sets.

5. Summary and Discussion

[25] Three legacy seismic sections west of the Iberian Peninsula have been reprocessed to extract and study physical oceanographic information contained in sound reflections within the water column. All sections show, in the depths between 200 and 2000 m, a large number of horizontally more or less continuous linear features that are reflective to seismic sound waves. In our data the sound reflection is caused by locally elevated vertical temperature gradients of at least a few hundredths of a degree over only a few meters [see also *Nandi et al.*, 2004]. These strong gradient layers are visible as thermohaline steps in conventional hydrographic data and are thought to be maintained by intrusive and/or double diffusive processes. Since these layers have been found to be rather stable over long periods and the double diffusive processes are typically rather slow, one can assume that they can be reversibly displaced in the vertical by internal waves. With seismic data, which often covers dozens of kilometers over a single day, it is thus possible to map the vertical displacement of reflectors or, in other words, it is possible to image internal wave displacement fields.

[26] We want to note here that besides internal waves, subinertial motions could contribute to the vertical displacement field. Such motions may for example be created in response to isolated diapycnal mixing events [*Sundermeyer and Ledwell*, 2001]. An analysis of data from the North Atlantic Tracer Release Experiment (NATRE) showed that subinertial motions have dominant horizontal and vertical wavelengths of about 1.2 km and 15 m, respectively [*Polzin et al.*, 2003; *Polzin and Ferrari*, 2004] and contribute thus to the spectral range analyzed here.

[27] In this study we applied spectral analysis to the displacement fields. The analysis results in wave number spectra similar to those obtained by a towed sensor package [*Katz and Briscoe*, 1979] but with a near continuous coverage over a good part of the water column and over long sections. This enables us to calculate the vertically averaged power spectral density of internal wave displacement along the three legacy sections. The resulting spectra are similar to those obtained by *Holbrook and Fer* [2005] off the Norwegian coast and agree quite well with Garrett-Munk internal wave spectra. All three sections show some spatial variability of the internal wave energy level as well as differences among them. Because of the limited number of reflectors only averages over relatively large subsections yield significant variations.

[28] The southernmost section IAM-4 is divided by Gorringe Bank and, in one half of the section, slices through a Meddy. On the Meddy's side the derived internal wave energy level is nearly twice as high as on the other side. One must, however, for multiple reasons be cautious when interpreting vertical displacements of reflectors in and near a Meddy. An underlying assumption of the Garrett-Munk model for internal waves, isotropic conditions, is certainly not true in a rotating Meddy. This rotation is also responsible for a wrapping of thermohaline intrusions around the Meddy's body. Such wrapped intrusive structures might appear as undulating reflectors when cut by seismic sections. Without a three-dimensional image of the reflectors it is, however, difficult to properly interpret the structures.

[29] As a higher energy level is found over the whole half of the section and not only close to the body of the Meddy, we may exclude the direct effect of the Meddy's interleaving with the surrounding water masses as possible cause. The possibility of the generation of internal waves radiating away from the Meddy also seems to be very unlikely. Near-inertial wave energy that may be trapped in anticyclonic vortices as shown for a Gulf Stream warm-core ring was found to be lost mainly to turbulence. Untrapped internal waves, able to leave the region of the eddy, received only a negligible part of the available energy [*Kunze et al.*, 1995]. Enhanced subinertial motions in the vicinity of the Meddy as discussed above may contribute to the enhanced energy level. However, without additional hydrographic and current data we are not able to address the Meddy's role for variations in the vertical displacement field. We only note here a higher energy level north of Gorringe Bank.

[30] Section ISE-12 crosses another regional topographic feature, Galicia Bank. Twice along that section the sea floor rises to less than 3000 m and exhibits a rougher topography. Even though the sea floor remains well below the layer of reflections a significant energy level difference between the shallow and deep parts is apparent in the data. The third section, ISE-17, is located further north on the east side of Galicia Bank. Again we find higher energy levels in the shallower parts of the section.

[31] In summary we show that the level of internal wave energy can be determined from seismic data and can be compared among different sections and even to some extent within a single section. In our data we were able to document significant variations of the energy levels that appear to depend on topography and hydrographic circumstances. The tools developed for this study can easily be applied to other seismic sections. The analysis of more legacy sections, which typically need to be reprocessed in order to extract the water column data, should lead to a better understanding of the relationships suggested from this data.

[32] **Acknowledgments.** We would like to thank Steve Holbrook and one anonymous reviewer for their helpful comments. The authors received support from the Deutsche Forschungsgemeinschaft under grant KR 3488/1-1 and from the European Union project GO under grant 15603 (NEST).

References

Banda, E., M. Torné, and I.A.M. Group (1995), Iberian Atlantic margins group investigates deep structure of ocean margins, *Eos Trans. AGU*, *76*, 25–32.

Bower, A. S., L. Armi, and I. Ambar (1997), Lagrangian observations of Meddy formation during a Mediterranean undercurrent seeding experiment, *J. Phys. Oceanogr.*, *27*, 2545–2575.

Garrett, C., and W. Munk (1975), Space-time scales of internal waves: A progress report, *J. Geophys. Res.*, *80*(3), 291–297.

Guo, N., and S. Fagin (2002), Becoming effective velocity-model builders and depth imagers. part II: The basics of velocity-modeling building, examples and discussion, *Leading Edge*, *21*(12), 1210–1216.

Holbrook, W. S., and I. Fer (2005), Ocean internal wave spectra inferred from seismic reflection transects, *Geophys. Res. Lett.*, *32*, L15604, doi:10.1029/2005GL023733.

Holbrook, W. S., P. Paramo, S. Pearse, and R. W. Schmitt (2003), Thermohaline fine structure in an oceanographic front from seismic reflection profiling, *Science*, *301*, 821–824.

Johannessen, O. M., and O. S. Lee (1974), A deep stepped thermohaline structure in the Mediterranean, *Deep Sea Res.*, *21*, 629–639.

Katz, E. J., and M. G. Briscoe (1979), Vertical coherence of the internal wave field from towed sensors, *J. Phys. Oceanogr.*, *9*, 518–530.

Kunze, E., R. W. Schmitt, and J. M. Toole (1995), The energy balance in a warm-core ring's near-inertial critical layer, *J. Phys. Oceanogr.*, *25*, 942–957.

Levitus, S., and T. Boyer (1994), *World Ocean Atlas 1994 Volume 4: Temperature*, NOAA Atlas NESDIS 4, Department of Commerce, Washington, D.C.

Magnell, B. (1976), Salt fingers observed in the Mediterranean outflow region (34°N, 11°W) using a towed sensor, *J. Phys. Oceanogr.*, *6*, 511–523.

May, B. D., and D. E. Kelley (2002), Contrasting the interleaving in two baroclinic ocean fronts, *Dyn. Atmos. Ocean.*, *36*, 23–42.

Merryfield, W. J. (2002), Intrusions in double-diffusively stable arctic waters: Evidence for differential mixing?, *J. Phys. Oceanogr.*, *32*, 1452–1459.

Nandi, P., W. S. Holbrook, S. Pearse, P. Paramo, and R. W. Schmitt (2004), Seismic reflection imaging of water mass boundaries in the Norwegian Sea, *Geophys. Res. Lett.*, *31*, L23311, doi:10.1029/2004GL021325.

Pérez-Gussinyé, M., C. R. Ranero, T. J. Reston, and D. Sawyer (2003), Mechanisms of extension at nonvolcanic margins: Evidence from the Galicia interior basin, west of Iberia, *J. Geophys. Res.*, *108*(B5), 2245, doi:10.1029/2001JB000901.

Polzin, K., and R. Ferrari (2004), Isopycnal dispersion in NATRE, *J. Phys. Oceanogr.*, *34*, 247–257.

Polzin, K. L., E. Kunze, J. M. Toole, and R. W. Schmitt (2003), The partition of finescale energy into internal waves and subinertial motions, *J. Phys. Oceanogr.*, *33*, 234–248.

Sundermeyer, M., and J. Ledwell (2001), Lateral dispersion over the continental shelf: Analysis of dye release experiments, *J. Geophys. Res.*, *106*(C5), 9603–9621.

Warner, M. (1990), Absolute reflection coefficients from deep seismic reflections, *Tectonophysics*, *173*, 15–23.

P. Brandt, D. Klaeschen, and G. Krahmann, Leibniz-Institut für Meereswissenschaften an der Universität Kiel, IFM-GEOMAR, D-24105 Kiel, Germany. (gkrahmann@ifm-geomar.de)

T. Reston, School of Geography, Earth and Environmental Sciences, University of Birmingham, B15 2TT, Birmingham, U.K.